

Near wall hemodynamics: modelling the glycocalyx and the endothelial surface

Giuseppe PONTRELLI^{1,*}, Ian HALLIDAY², Tim J. SPENCER², Chris M. CARE¹,
Carola S. KÖNIG³, Michael W. COLLINS⁴

*Corresponding author: Tel.: +39 (0)6 49270927; Fax: +39 (0)6 4404306;

Email: giuseppe.pontrelli@gmail.com

¹Institute for Applied Computing, CNR, Italy

²Materials and Engineering Research Institute, Sheffield Hallam University, Sheffield, UK

³Institute for Bioengineering, Brunel University, UK

⁴School of Engineering and Design, Brunel University, UK

Abstract: In this paper a coarse-grained model for blood flow in small arteries is presented. Blood is modelled as a two-component incompressible fluid: the plasma and corpuscular elements dispersed in it. The latter are modelled as deformable liquid droplets having greater density and viscosity. Interfacial surface tension and membrane effects are present to mimic key properties and to avoid droplets' coalescence. The mesoscopic model also includes the presence of the wavy wall, due to the endothelial cells and incorporates a representation of the glycocalyx, covering the vessel wall. The glycocalyx is modelled as a porous medium, the droplets being subjected to a repulsive elastic force when approaching it, during their transit. Preliminary simulations are intended to show the influence of the undulation on the wall together with that of the glycocalyx.

Keywords: microcirculation, glycocalyx, Lattice Boltzmann method, multi-component fluid, endothelium.

1. Introduction

The endothelium plays a number of important roles in the vascular system. Dysfunction or healing of endothelial cells may lead to several pathological states, including early development of atherosclerosis (Yao et al., 2007). The microscopic shape of the endothelium is defined by the presence of endothelial cells (ECs henceforth), making the arterial wall undulate. This effect becomes more pronounced in small-sized vessels, where the corrugation degree increases. The study of blood flow over a regularly undulating wall made of equally aligned and distributed EC's has been recently carried out by Pontrelli et al. (2011) who quantified the variation of wall shear stress over the EC's.

Furthermore, the endothelium is coated by long-chained macromolecules and proteins which form a thin porous layer, called *glycocalyx* (fig. 1). (Weinbaum et al., 2007). The glycocalyx has a "brushlike" structure and a thickness which varies with the vessel diameter, but its average is 100nm for arterioles. It has several roles: it serves as a transport barrier, to prevent ballistic red blood cell interactions with the endothelium, and as a sensor and transducer of mechanical forces,

such as fluid shear stress, to the surface of ECs. Actually, it has been recognized that the glycocalyx respond to the flow environment and, in particular, to the fluid stress, but the mechanism by which these cells sense the shearing forces and transduce mechanical into biochemical signals is still not fully understood (Weinbaum et al. 2007, Pahakis et al. 2007).



Fig 1. The "brushlike" structure of the glycocalyx over the wavy wall constituted by a sequence of equally aligned EC's (courtesy by Yao et al., 2007).

The glycocalyx itself is remodeled by the shearing flow and by the compression exerted by the deformed erythrocytes in capillaries (Secomb et al., 2002).

Flow induced mechano-transduction in EC's has been studied over the years with emphasis on correlation between disturbed flow and atherosclerosis. Recently, some mathematical modelling work has been carried out by Arslan (2007) and Vincent et al. (2008), using a porous medium to model the glycocalyx layer

(GL henceforth). However, none of these works includes the effect of the roughness, or wavy nature, of the wall, which is incorporated in our model for a realistic description.

In the following sections we present a coarse-grained model that attempts to include some of the basic physical microscale effects of the GL attached to the EC surface and hence, examine to what extent the wall shear stress may vary due to this layer in addition to the previously examined EC shape and particulate transport. To model blood flow in small-sized arteries, the mesoscopic lattice Boltzmann (LB) method is used. Our model includes a physical representation of the EC's shape through a wavy wall, a multi-component flow model of viscous fluid droplets with interfacial surface tension and, finally, a representation of the GL that considers both the effect upon the particles and the fluid transport properties.

2. Blood flow in arterioles

In nearly all studies of haemodynamics, blood is assumed to be an incompressible, Newtonian fluid, and the arterial wall to be flat. The first assumption ignores the non-Newtonian effect and the particulate nature of the blood, and the latter neglects the mesoscale undulation of the wall due to the shape of the influence of constituent EC's: this does not imply a significant variation in the flow field, but it can be relevant in computing WSS, which is constant in a flat-walled artery. Indeed, the internal surface of the vessel wall is covered by a sequence of EC's forming a continuous, wavy layer. A single EC has been estimated to be about $15 \mu m$ long by $0.5 \mu m$ high (Reichlin et al., 2005) (fig. 2). At such mesoscopic scale, the wall may be considered as a smoothly corrugated idealized surface constituted by a regular array of equal, repeated EC's. The pressure-driven axisymmetric flow of a continuum fluid over such a surface has been recently modelled by Pontrelli et al. (2011). It was shown that, despite no great change in velocity profiles, there can occur significant WSS variations between the wall peaks and throats, especially in small-sized arteries.

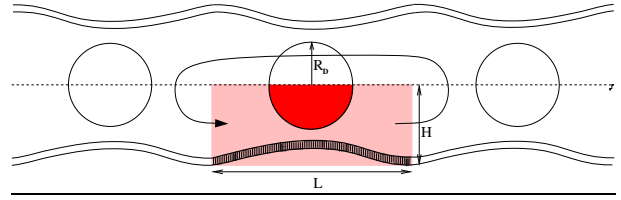


Fig. 2: Schematic diagram of our model system. Due to axisymmetry, only flow in a half-channel is considered. Further, even with the wall undulation we retain a periodicity condition, so only a portion of the vessel - corresponding to the size of an endothelial cell - is considered (gray region). The hatched layer near the wall indicates the glycocalyx, and the arrow line the inlet-outlet periodic boundary conditions implemented in our simulations (figure not to scale).

Extending this work, the particulate nature of the fluid is further included here, by considering the fluid plasma containing separated erythrocytes, modelled as deformable, neutrally buoyant liquid drops constrained by a uniform interfacial tension.

In the current formulation the erythrocytes are free to migrate away from the wall and their degree of deformation is much less than those geometrically constrained in capillaries (Secomb et al, 2002). We consider a 2D axisymmetric channel having the same corrugation repeated along the length, and semi-height H , much larger than the erythrocyte radius. For the sake of simplicity only one EC is considered and periodic boundary conditions are imposed in order to model a long enough channel (fig. 2). In a cartesian coordinate system (x,y) the domain is defined as $[0, L] \times [0, H]$. For simplicity, a single circular droplet of radius R_D is initially placed in the plasma, and centered on the system's symmetry line (fig. 2).

3. Glycocalyx modelling

As described above, the endothelial surface is not only wavy in its geometry, but, at a smaller scale, it is covered by fibrous filaments and long protein chains forming a thin layer called the *endothelial surface layer or glycocalyx*. From a fluid dynamics point of view, the GL may be modelled as a porous layer of constant thickness which follows the wall undulation,



Fig. 3: Assumed mechanical properties of the glycocalyx protein chains, subject to a streaming flow only (A) and direct, ballistic interaction with a particulate (B). Note that the principal deformation is assumed to be confined to the tip of the filaments, adjacent to the lumen (figure not to scale).

through which the flow of the continuous phase (plasma) is possible. This would alter the boundary condition of the problem, specifically the classical no-slip condition at the vessel wall may have to be replaced, to allow for plasma penetration through, say, the GL and endothelial clefts. The lattice Boltzmann (LB) method we employ here readily accommodates a model of the glycocalyx itself, as it is particularly well suited to address what would now become a multiscale model. Conceptually, the idea is to solve a two-domain problem, whereby the inner flow, or bulk flow (in the lumen) is governed by the Navier-Stokes equations, and in the near-wall region by a porous-medium Brinkmann flow formulation (see below).

At the mesoscale, the glycocalyx is not modelled in a detailed form, but its effect on the flow is still properly addressed, using methods which are amenable to coupling other, more detailed, simulations with experiments. We present here a “two-way coupled” model where the drop interface is forced by compression of GL, and the effect of perturbed or compressed GL is then communicated to the flow (fig. 3). We assume here that the filaments are strongly anchored in the endothelium, where they are most resistant to deformation and that they deform preferably at their tip i.e. towards the vessel lumen (fig. 3). The non-linear mechanical response of the GL to ballistic impact is a complex and challenging issue that must eventually be verified by experimental micro-scale studies.

4. Formulation of the problem

We use a mesoscale LB method to solve the governing hydrodynamic equations, that involves multi-component fluid flow, off-lattice, or sub-grid, boundary surfaces and a porous-layer representative of the GL. The governing hydrodynamic equations for flow in a porous media, with constant or variable porosity, $\varepsilon(\underline{x})$, as presented in Guo and Zhao (2002), are:

$$\nabla \cdot \underline{u} = 0 \quad (1)$$

$$\frac{\partial \underline{u}}{\partial t} + (\underline{u} \cdot \nabla) \left(\frac{\underline{u}}{\varepsilon} \right) = -\frac{1}{\rho} \nabla (\varepsilon P) + \nu \nabla^2 \underline{u} + \underline{F} \quad (2)$$

Here ρ , \underline{u} and P are the fluid density, velocity and pressure respectively and ν is the effective fluid viscosity. \underline{F} is the total body force due to the presence of both the porous material (drag) and other external forces, including that which we use to represent interfacial tension (Halliday et al, 2007):

$$\underline{F} = -\frac{\varepsilon \nu}{K} \underline{u} - \frac{\varepsilon F_\varepsilon}{\sqrt{K}} \underline{u} |\underline{u}| + \varepsilon \underline{G} \quad (3)$$

where $K = \frac{\varepsilon^3 d^2}{150(1-\varepsilon)^2}$ is the permeability, d is a property of the porous structure, and $F_\varepsilon = \frac{1.75}{\sqrt{150\varepsilon^3}}$ is a geometrical

function. \underline{G} is the extra body force that will be used to incorporate further details of the GL and particulate forces, such as the interface force density (Guo and Zhao, 2002) defined below.

To solve governing equations (1)-(3) and also include particulate components, we combine the lattice Boltzmann methods of Guo and Zhao (2002), with the model of Halliday et al. (2007), that allows for the introduction of two immiscible fluid components and the formation of interfaces that embed correct kinematic and surface tension laws. Following

the notations of those papers, the resultant LB algorithm for the particle distribution functions, $f_i(\underline{x}, t)$, at position \underline{x} , time t and lattice link direction i , is written as an evolution process comprised of a collision:

$$f_i^+ = f_i(\underline{x}, t + \Delta t) = f_i(\underline{x}, t) - \frac{1}{\tau} (f_i(\underline{x}, t) - f_i^{eq}(\underline{x}, t)) + \Delta t F_i$$

and a propagation, to be discussed below. In the last equation, the equilibrium distribution function, f_i^{eq} , and lattice source term, F_i , are defined, respectively, as

$$f_i^{eq}(\underline{x}, t) = t_i \rho \left(1 + \frac{\underline{e}_i \cdot \underline{u}}{c_s^2} + \frac{\underline{u} \underline{u} (\underline{e}_i \underline{e}_i - c_s^2 \underline{I})}{2\epsilon c_s^4} \right)$$

$$F_i(\underline{x}, t) = t_i \rho \left(1 - \frac{1}{2\tau} \right) \left[\frac{\underline{e}_i \cdot \underline{F}}{c_s^2} + \frac{\underline{u} \cdot \underline{F} (\underline{e}_i \underline{e}_i - c_s^2 \underline{I})}{\epsilon c_s^4} \right]$$

In these equations \underline{I} is the identity matrix, \underline{e}_i and t_i are the lattice basis vectors and associated weights, c_s is the speed of sound of the LB model lattice used, and τ is a relaxation parameter, related to the fluid viscosity (Succi, 2001). The density, ρ , final velocity, \underline{u} , fluid pressure, P , and kinematic viscosity, ν , in our particular LB model, are expressed, in lattice units, respectively as:

$$\rho = \sum_i f_i(\underline{x}, t)$$

$$\underline{u} = \frac{\underline{v}}{p_0 + \sqrt{p_0^2 + p_1 |\underline{v}|}}$$

$$P = \rho c_s^2$$

$$\nu = \frac{\Delta t c_s^2}{2} (2\tau - 1)$$

in which the following auxiliary quantities are defined (Guo and Zhao, 2002):

$$\rho \underline{v} = \sum_i \underline{e}_i f_i(\underline{x}, t) + \frac{\Delta t}{2} \epsilon \rho \underline{G}$$

$$p_0 = \frac{1}{2} \left(1 + \frac{\epsilon}{2} \frac{\nu}{K} \right)$$

$$p_1 = \left(\frac{\epsilon}{2} \frac{F_\epsilon}{\sqrt{K}} \right)$$

To complete our account of the LB algorithm, we must mention that the, for multiple fluid LB, the propagation step is augmented by a fluid segregation process (Halliday et al. 2007) that ensures the correct kinematics and dynamics and good integrity for an interface between completely immiscible fluid components, representing our particulates, as discussed above. The propagation step is expressed as

$$R_i(\underline{x} + \underline{e}_i \Delta t, t + \Delta t) = \frac{R}{\rho} f_i^+ + t_i \beta \frac{RB}{\rho} \hat{n} \cdot \underline{e}_i$$

$$B_i(\underline{x} + \underline{e}_i \Delta t, t + \Delta t) = \frac{B}{\rho} f_i^+ - t_i \beta \frac{RB}{\rho} \hat{n} \cdot \underline{e}_i \quad (4)$$

where the density of each fluid component is given by $R = \sum_i R_i(\underline{x}, t)$ and

$B = \sum_i B_i(\underline{x}, t)$ and the combined particle distribution function

is $f_i(\underline{x}, t) = R_i(\underline{x}, t) + B_i(\underline{x}, t)$, β is an interfacial segregation parameter and \hat{n} is an interfacial unit normal vector. We also note that, if only one fluid component exists, eqs. (4) reduce to the standard lattice Boltzmann propagation step.

Returning to the definition of the extra body force term, \underline{G} in eq. (3), this incorporates both particulate and glycocalyx forces and is defined as

$$\underline{G} = \frac{\sigma}{2\rho} \pi \nabla \rho_N + \underline{E}$$

The left hand side term imposes an interfacial tension, σ , on multicomponent particles. Here $\pi = \nabla \cdot \hat{n}$ is the local curvature and $\rho_N = (R - B)/(R + B)$ is a phase field indicator. The right hand term, \underline{E} , is a glycocalyx force that acts upon the particles as defined in the next section.

For practical purposes the off lattice non-slip endothelial surface uses continuous bounce back conditions (Bouzidi et al. 2001). A pressure driven flow U is imposed at the inlet-

outlet, as periodic boundary conditions (Kim and Pitsch, 2007). The shape of the endothelial cell is assumed as that measured by Reichlin et al. (2005).

5. Erythrocytes-glycocalyx interaction

In the proposed model of the GL as a porous layer, the porosity is reduced by a compressive encounter with an erythrocyte. As a consequence, GL is squashed locally, transporting the same mass into a smaller volume, and consequently decreasing the porosity in that region. Even in the simplest situation, the GL-lumen boundary should not be regarded as sharp and there is an “uncertainty” region between bulk, lumen and glycocalyx material. Let us define a variable porosity $\varepsilon(x,y)$ that tends to 1 in the lumen region and gradually reduces, as we enter the glycocalyx region, where it approaches a minimum value, ε_G . This porosity transition is modelled through the increasing smooth function:

$$\varepsilon(x, y) = \varepsilon_G + \frac{1 - \varepsilon_G}{2} [1 + \tanh[\xi(s - l)]] \quad (5)$$

where l is the mean GL thickness and the parameter $1/\xi$ determines the distribution of (i.e. the effective standard deviation of) protein chain lengths, while $s(x,y)$ denotes distance measured in the direction perpendicular to the endothelial boundary. Note that $\varepsilon_G \leq \varepsilon(x,y) \leq 1$ (fig. 4) and that for $\varepsilon \rightarrow 1$ we have $\underline{F} \rightarrow \underline{G}$ and the equations (1)-(3) reduce to the multi-component LB Navier-Stokes equations for free multi-component fluid flows, and the described procedure reduces to the standard LBE for two-component, incompressible fluid. On the other hand, an additional, fictitious, repulsive body force density acts on the drop interface which enters the GL region, impinging on the lumen. This force distribution is so designed that its accumulation produces an effective Hookean force acting at the centre of the local volume. Specifically, the “erythrocyte”, the red fluid, is subjected to a surface force distribution,

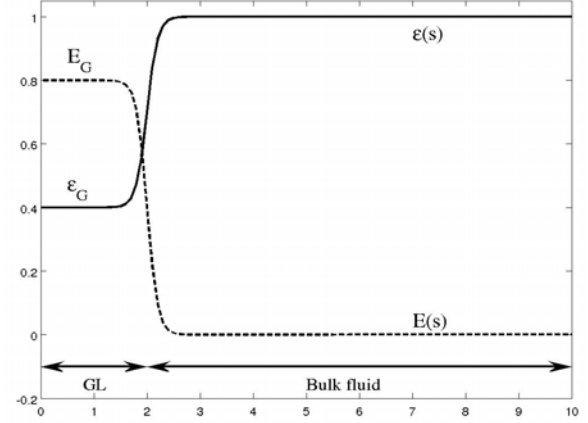


Fig. 4: The porosity function (continuous line) as a function of s : the latter increases from a minimum value ε_G (in the GL), to the bulk fluid ($\varepsilon=1$) (see eqn. (5)). Similarly the elasticity modulus E (dashed line) varies from a maximum value E_G in the GL to 0 (no elastic force) out of it (see eqn. (6)). Note, the smooth transition area (due to the uncertain GL thickness) that is controlled by the parameter ξ (figure not to scale).

effective in the GL only, which is directed everywhere in the drop-surface normal direction. This force device effectively models the glycocalyx as a continuum of elastic springs, with modulus E , gradually decaying from a maximum value, E_G , (in the GL) to 0 towards the bulk:

$$E(x, y) = \frac{E_G}{2} [1 - \tanh[\xi(s - l)]] \quad (6)$$

where all notations are given in correspondence to eqn. (5) (see fig 4). It is important to note that the above force acts solely on the red fluid (drop) and not upon the blue plasma. Hence, the relative density of the material which comprises the drop may be modelled by appropriate choice of the spring constant E_G in the above equation.

6. Numerical results and discussion

From the above, it is clear that the simulation depends on several parameters. Some relate to the key physical, geometrical or physiological details in the model (and all are, in principle, obtainable from experiments, note). For present purposes, we take:

$$L=300, \quad H=75, \quad U=0.03, \quad \nu=0.25, \quad R_D=60$$

(all in LB units), while the porous medium coefficients used are those given as in Guo and Zhao (2002). Since, in the present application, the fluid velocity is quite small, we neglect the nonlinear drag term and eqn. (1)-(3) reduce to the Brinkmann-extended Darcy equation.

All the above parameters combine to give the following nondimensional Reynolds and Darcy numbers:

$$Re = \frac{2UH}{\nu} = 18, \quad Da \approx 10^{-4}$$

Certain other parameters are artefacts of the numerical method of our ‘‘coarse-grained’’ mesoscale glycolyx modelling. They are thus designated as ‘‘microscopic’’ and quantified as follows:

$$\xi = 3, \quad l = 10, \quad E_G = 0.1, \quad \varepsilon_G = 0.6$$

Of course, all of the latter might be estimated by fitting experimental / microscale simulation data. For example, the standard deviation ξ could be measured from a representative sample of protein chain lengths, l , obtained from microscope images; the effective elasticity constant from fits to explicit microscale simulation data.

All the above parameters are chosen to simply produce an observable effect on the flow in the region of the drop, and must be correctly identified (or at least bounded within an appropriate range) to produce reliable simulations. We are aware that they are critically related to each other, and a suitable calibration of the set should be performed along with comparisons with experiment to produce realistic simulation outcomes.

It is important to note that the stability of simulations may be affected by the combination of the parameters as chosen, which limits the available parameter space for simulation. However, our tests indicate an encouragingly robust simulation system, with a large and accessible parameter space,

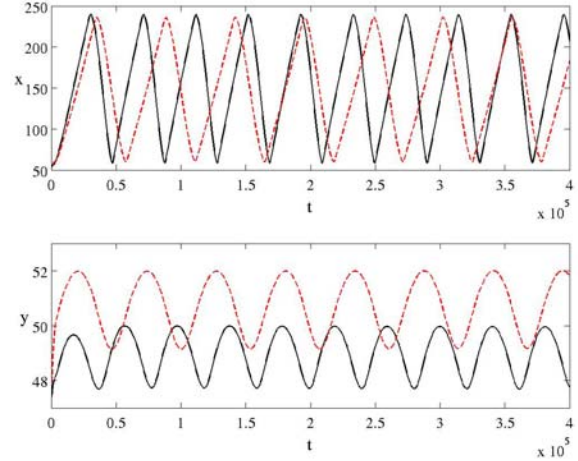


Fig. 5: Center of mass coordinates (x,y) of the drop half plane as a function of time, without any porous media or applied force (continuous black), and with porous media and applied forces (dashed red). In the latter case, the reduced slope of $x(t)$ (in a transit segment) estimates the droplet’s decreased mean speed and the greater value of $y(t)$ indicates a lifting of the droplet over the GL.

probably as a consequence of the small Re . The classical LB D2Q9 lattice scheme (Succi, 2001) in a multi-component form (Halliday et al., 2007) is chosen with the following parameters:

$$\tau = 1.25, \quad \rho = 1.8, \quad \beta = 0.67$$

We shall consider the effect of varying the glycolyx parameters, choosing the elastic coefficient E (see eqn. (6)), and the porosity function ε (see eqn. (5)).

As one may expect, the average velocity of the drop is slower in the presence of the glycolyx, which constitutes a hindrance for the lumen flow. Fig. 5 illustrates this fact. Also, the mean deformation of the drop is more pronounced in the presence of the glycolyx force (fig. 6). This is apparent in the difference between the average y coordinates recorded for the drops with and without the glycolyx force present. Hence, when the drop is in the GL influence region, it is subjected to the elastic force, which squeezes and lifts it, away from the boundary, whilst making its shape more elongated (fig.

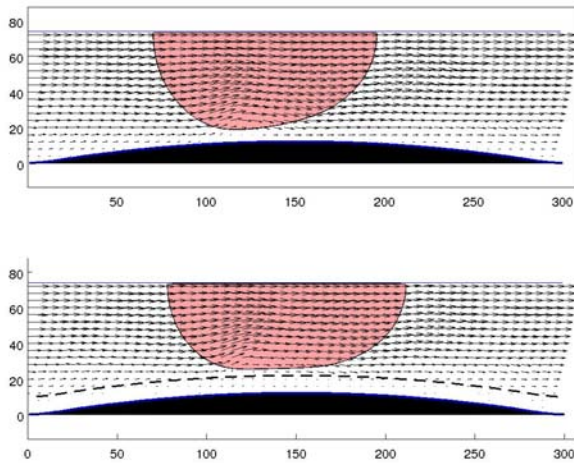


Fig. 6: The velocity field for the ‘aggregate’ fluid (drop and supernatant fluids combined) in the region of the endothelium. The extent of the GL is indicated by the broken line. It appears that an enhanced recirculation region is induced by the porous media perturbation (bottom), with respect to an experiment without glyocalyx (top). The glyocalyx force field density is most intense in the GL. The single deformable drop has been acted on by encountering the glyocalyx body force field. The flow refers to the same time ($t = 340000$ LB units) and appears to be deflected up which would tend to protect the endothelial cell surface from increased WSS.

6). Considering the action of the glyocalyx as a sensor of mechanical forces, it is worth computing the shear stress at the GL / lumen boundary (GSS). Fig. 7 shows the differences for WSS in the cases without and with glyocalyx: it evidences, in the latter case, a reduction of the shearing stress either at the wall (WSS, due to the plasma only) and at the GL top (GSS, due to the particulate fluid). It is possible that GL would be more likely to protect the endothelial cells from WSS fluctuations associated with particle transits.

7. Conclusions

Recent work has revealed a correlation between the flow-induced mechano-transduction in glyocalyx and the development of atherosclerosis. The presence of the glyocalyx is supposed necessary for the endothelial cells to respond to fluid shear, and

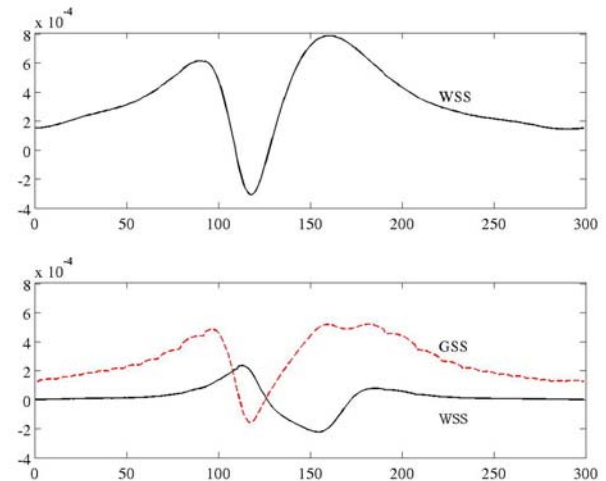


Fig. 7: The WSS and GSS along the channel at the same time ($t = 340000$ LB units, cfr. fig. 6), without (top) and with glyocalyx (bottom).

its role is characterized by studying its response to fluid shear stress.

A coarse-grained model and a preliminary numerical simulation of the blood flow over a wavy wall, covered by a prototype GL has been proposed here. The most pressing consequence of our modelling assumptions, as set out above, is the need to formulate some theory of the relationship between the way in which protein chains are compacted and the effect of this process on the effective viscosity. There are several ways one might approach this problem. We favour a direct numerical solution of the full Navier-Stokes / continuity equations, of incompressible flow through a channel packed with a variable volume fraction of solid filamentary structures and subsequent modelling of their effect on average channel discharge. A better but very much more computationally-demanding approach to assessing the local glyocalyx-induced flow perturbation would involve coupling to a sub-grid distribution of anchored, point particles, which could disrupt or impede flow. By making the local concentration of these ‘scattering centres’ proportional to the local glyocalyx compression, a more accurate and physically correct representation of the glyocalyx might be achieved. Similar arguments around the calibration of this model as discussed in the above paragraph apply. Future developments

will concern the extension to 3D cases, based upon parallel codes, and to larger particle concentrations. The latter problem is essentially solved (Spencer et al. 2011), however it requires significant software development efforts to install it alongside the boundary conditions used in this work. Another direction we are undertaking is to enhance our current, simplistic, interfacial tension model with additional stresses and bending properties associated with elastic membranes, such as those in Secomb et al (2002). The applicability of the present model is restricted to simple flow problems. Our next effort is to modify and extend the behaviour our fluid-fluid interface so as to enrich and adapt its existing mechanical properties, in a manner which mimics the thin membrane of erythrocytes.

References

- Arslan, N., 2007, Mathematical solution of the flow field over glycocalyx inside vascular system, *Math. Comp. Appl.*, 12(3), 173-179.
- Bouzidi, M., Firdaouss, M., Lallemand, P., 2001, Momentum transfer of a Boltzmann-lattice fluid with boundaries, *Phys. Fluids* 13(11), 3452-3459.
- Guo, Z. and Zhao, T.S., 2002, Lattice Boltzmann model for incompressible flows through porous media, *Phys. Rev. E*, 66, 036304.
- Halliday, I., Hollis, A.P., Care, C.M., 2007, Lattice Boltzmann algorithm for continuum multicomponent flow, *Phys. Rev. E*, 76, 026708.
- Kim, S.H. and Pitsch, H., 2007, A generalized periodic boundary condition for lattice Boltzmann method simulation of a pressure driven flow in a periodic geometry, *Phys. Fluids*, 19, 108101.
- Pahakis, M.Y., Kosky, J.R., Dull, R.O., Tarbell, J.M., 2007, The role of endothelial glycocalyx components in mechanotransduction of fluid shear stress, *Biochem. Biophys. Res. Comm.*, 355(1), 228-233.
- Pontrelli, G., Köenig, C.S., Halliday, I., Spencer, T.J., Collins, M.W., Long, Q., Succi, S., 2011, Modelling wall shear stress in small arteries using the Lattice Boltzmann method: influence of the endothelial wall profile, *Med. Eng. Phys.*, on line, doi:10.1016/j.medengphy.2011.03.009
- Reichlin, T., Wild, A., Dürrenberger, M., Daniels, A.U., Aebi, U., Hunziker, P.R., Stolz, M., 2005. Investigating native coronary artery endothelium in situ and in cell culture by scanning force microscopy. *J. Structural Biol.*, 152, 52-63.
- Secomb T.W., Hsu, R, Pries, A.R., 2002, Blood flow and red blood cell deformation in nonuniform capillaries: effects of the endothelial surface layer, *Microcirculation* 9, 189-196.
- Spencer, T. J., Halliday, I. Care, C.M., 2011, A local lattice Boltzmann method for multiple immiscible fluids and dense suspensions of drops. *Phil. Trans. R. Soc. A* 369, 2255-2263.
- Succi, S., 2001, Lattice Boltzmann equation for fluid dynamics and beyond, Oxford Univ. Press.
- Vincent, P.E., Sherwin, S.J., Weinberg, P.D., 2008, Viscous flow over outflow slits covered by an anisotropic Brinkman medium: a model of flow above interendothelial cell cleft, *Phys. Fluids*, 20(6), 063106.
- Weinbaum, S., Tarbell, J.M., Damiano, E.R., 2007, The structure and the function of the endothelial glycocalyx layer, *Ann. Rev. Biom. Eng.*, 9, 6.1.
- Yao, Y., Rabodzey, A, Forbes Dewey Jr., C., 2007, Glycocalyx modulates the motility and proliferative response of vascular endothelium to fluid shear stress, *Am. J. Physiol. Heart Circ. Physiol.* 293:H1023-H1030.